Effective charges and virial pressure of concentrated macroion solutions

Niels Boon[a], Guillermo Ivan Guerrero-García[a,b], René van Roij[c], and Monica Olvera de la Cruz[a,1]

[a]Department of Materials Science and Engineering, Northwestern University, Evanston, IL 60208; [b]Instituto de Física, Universidad Autónoma de San Luis Potosí, 78000 San Luis Potosí, Mexico; and [c]Institute for Theoretical Physics, Center for Extreme Matter and Emergent Phenomena, Utrecht University, 3584 CE Utrecht, The Netherlands

The stability of colloidal suspensions is crucial in a wide variety of processes, including the fabrication of photonic materials and scaffolds for biological assemblies. The ionic strength of the electrolyte that suspends charged colloids is widely used to control the physical properties of colloidal suspensions. The extensively used two-body Derjaguin–Landau–Verwey–Overbeek (DLVO) approach allows for a quantitative analysis of the effective electrostatic forces between colloidal particles. DLVO relates the ionic double layers, which enclose the particles, to their effective electrostatic repulsion. Nevertheless, the double layer is distorted at high macroion volume fractions. Therefore, DLVO cannot describe the many-body effects that arise in concentrated suspensions. We show that this problem can be largely resolved by identifying effective point charges for the macroions using cell theory. This extrapolated point charge (EPC) method assigns effective point charges in a consistent way, taking into account the excluded volume of highly charged macroions at any concentration, and thereby naturally accounting for high volume fractions in both salt-free and added-salt conditions. We provide an analytical expression for the effective pair potential and validate the EPC method by comparing molecular dynamics simulations of macroions and monovalent microions that interact via Coulombic potentials to simulations of macroions interacting via the derived EPC effective potential. The simulations reproduce the macroion–macroion spatial correlation and the virial pressure obtained with the EPC model. Our findings provide a route to relate the physical properties such as pressure in systems of screened Coulomb particles to experimental measurements.

colloids | DLVO | macroions | electrolytes | cell model

Coulombic interactions between ionized species affect colloidal suspensions at the microscopic level and have an indirect, yet crucial, impact on the observable macroscopic characteristics of the system (1). The Derjaguin–Landau–Verwey–Overbeek (DLVO) theory (2, 3), proposed in the 1940s, has been crucial for understanding like-charged colloidal dispersions in a wide variety of experimental conditions. In this theory, the effective pair potential between two equally charged macroions immersed in an electrolyte is expressed as the sum of three terms: a hard-core potential that takes into account the excluded volume of macroions (preventing their overlap), an attractive potential due to short-range (van der Waals) interactions, and an electrostatic screened Coulomb or Yukawa potential resulting from the linearized Poisson–Boltzmann theory, which is the Debye–Hückel approximation. Many additions and modifications to the original theory have been proposed, including polarization effects, patchiness, or charge regulation, just to mention a few. Special care should be taken for nonaqueous solvents, divalent ions, or high salt concentrations, since, in these regimes, ion correlations are usually important (4–16). Generally speaking, modifications to the DLVO theory have been pivotal for systems in which the electrostatics are not well described by the linearized Poisson–Boltzmann (PB) theory. Although the DLVO theory has been used extensively to model colloidal dispersions (17), this approach

is not exact within the context of the underlying Debye–Hückel approximation. In the precise analysis of the force between two charged spheres in an electrolytic solution, Verwey and Overbeek encountered additional terms that can be considered cross terms, resulting from the exclusion of the ionic double layer surrounding the first sphere by the hard core of the second sphere (3). Numerical methods exist to quantify such effects (18–20), yet these approaches explicitly deal with two particles in an otherwise empty system. While in dilute solutions of macroions the resulting correction to DLVO is typically small and can usually be safely neglected, in dense macroion systems, the deviation from DLVO can become very significant due to the overlap between each macroion electrical double layer with the hard cores of all neighboring particles. As a result, the performance of the classical DLVO equation is limited to the description of dilute systems of macroions (21–25), while many colloidal processes such as crystallization or glass formation predominantly occur in dense systems where many-body effects prevail. Marcelja et al. recognized the importance of many-body effects at high colloidal densities and low electrolyte concentration, and they described a method that uses cell theory to project a charged colloidal dispersion to a system of Coulomb particles (26). This enabled use of Monte Carlo simulations of the Wigner lattice to study the crystallization of latex suspensions. That method has recently been rediscovered and extended to charge-regulating particles to describe reentrant melting on addition of a charging agent to a colloidal suspension (27). Such an effective Coulomb representation is, however, not suitable to describe the structure of charged suspensions, particularly in the

Significance

Colloids constitute the basic components of many everyday products and are integrated into the fabric of modern society. Understanding their assembly is key for nanotechnological and biotechnological advances. At the single-particle level, colloids commonly possess electric charge. Consequently, the structure to which they conform is strongly influenced by electrostatic interactions. In solution, these interactions are modified by the presence of ions. We have developed a model for computing the corresponding effective electrostatic interactions as well as the osmotic pressure. Our model extends the applicability of Derjaguin–Landau–Verwey–Overbeek theory to dense systems in which many-body effects are crucial. This will allow previously impossible, mesoscale studies of colloidal assembly to be performed analytically or by simulation with implicit ions models.

crystalline phase. This is also true of methods comprising the repulsive forces among macroions via hard-sphere interactions with effective hard-sphere radii (28–31). Different approaches such as the (renormalized) Jellium model (32) and methods that calculate the osmotic pressure within a Wigner–Seitz cell (33, 34) have been proposed. However, they do not yield information on the spatial configuration of the macroions and consequently are limited in describing dense macroion systems.

Model

In this work, we introduce a method to calculate the effective electrostatic pair interaction between macroions in dense systems through the identification of their corresponding effective point charges. We verify the corresponding accuracy by comparing the resulting radial distribution functions and pressures to the primitive model (PM). To begin, we consider spherical and impenetrable macroions of valence Z and radius a immersed in a 1:1 electrolyte with bulk concentration c_s. Traditionally for dilute macroion systems, the nonlinear PB theory establishes that the electrostatic potential is described by $\nabla^2 \Phi(\mathbf{r}) = \kappa_{\mathrm{res}}^2 \sinh \Phi(\mathbf{r})$ outside the macroion, where $\Phi(\mathbf{r}) = \Psi(\mathbf{r}) e / k_B T$, $\Psi(\mathbf{r})$ is the electrostatic potential, e is the elementary charge, and $k_B T$ is the thermal energy of the solution. The parameter $\kappa_{\mathrm{res}} = \sqrt{8\pi \lambda_B c_s}$ is an inverse screening length depending on the Bjerrum length $\lambda_B \equiv e^2/(k_B T \epsilon)$, where ϵ is the relative dielectric permittivity. For sufficiently small charges, the PB equation can be linearized by using $\sinh \Phi(\mathbf{r}) \approx \Phi(\mathbf{r})$, resulting in the Debye–Hückel approximation, $\nabla^2 \Phi(\mathbf{r}) = \kappa_{\mathrm{res}}^2 \Phi(\mathbf{r})$. The electrostatic potential outside the macroion is found to be $\Phi(r) = \lambda_B Q_{\mathrm{DLVO}} \exp(-\kappa_{\mathrm{res}} r)/r$, with $r > a$ the distance to the center of the particle and $Q_{\mathrm{DLVO}} \equiv Z \exp(\kappa_{\mathrm{res}} a)/(1 + \kappa_{\mathrm{res}} a)$. The electric field, and thus the electrostatic force it exerts on a test charge (35), is the same as that of a point particle with charge Q_{DLVO}. One can therefore identify Q_{DLVO} as the effective point charge in the DLVO theory and estimate the pair potential between two macroions from the screened Coulomb interaction of two point charges at a distance D,

$$\frac{U(D)}{k_B T} = Q^2 \lambda_B \frac{\exp(-\kappa D)}{D}, \qquad [1]$$

with $Q = Q_{\mathrm{DLVO}}$ and $\kappa = \kappa_{\mathrm{res}}$ according to DLVO theory.

Apart from being restricted to dilute systems, the DLVO equation above cannot directly be applied to strongly charged macroions, since the Debye–Hückel approximation no longer holds for these systems, which, strictly speaking, leads to nonpairwise additive interaction potentials (36, 37). Alexander et al. (33), however, showed that nonlinear ion behavior close to the macroion surface can be embodied in an effective linear screening model by calculating a renormalized surface charge Z^* that, far away from the charged macroion surface, induces the same electrostatic potential and electric field as would be obtained within the nonlinear PB equation (33, 38–42); see Fig. 1F. Regarding a system of macroions at a concentration ρ_M and macroion packing fraction $\eta = 4\pi \rho_M a^3/3$, each of the macroions is imagined to be in the center of a charge-neutral spherical cell with radius $R = a\eta^{-1/3}$, such that the summed volume of all cells matches the system's volume (21). This is illustrated in Fig. 1C. In this spherical geometry, the nonlinear PB equation and the associated boundary conditions can be written as

$$\Phi''(r) + \frac{2\Phi'(r)}{r} = \kappa_{\mathrm{res}}^2 \sinh \Phi(r) \qquad [2a]$$

$$\Phi'(a) = -\frac{Z\lambda_B}{a^2}; \quad \Phi'(R) = 0, \qquad [2b]$$

where the prime denotes a derivative with respect to r. The boundary conditions follow from Gauss' law and include the global
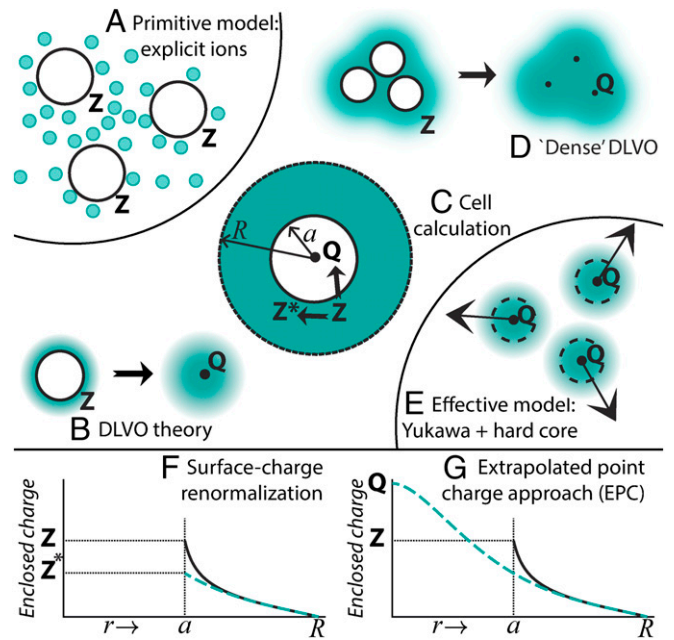

Fig. 1. The various paths (*B–D*) from the PM (*A*) of monovalent microions and macroions of valency Z to the effective model (*E*) where interactions are hard-core Yukawa with effective point charges Q. (*F* and *G*) PB cell calculations for the electric field (or charge within radius r) around a macroion following from nonlinear calculations (full line) and the Debye–Hückel fit (dashed line); *F* illustrates how surface charge renormalization yields a charge Z^* that can be inserted into DLVO theory. In the EPC approach, the effective point charge Q is calculated directly from the extrapolation displayed in *G*.

electroneutrality condition of the whole system. This set of equations is typically solved numerically, as no general analytical solution is known. Once the numerical solution is determined, one proceeds by linearizing Eq. **2a** around the obtained potential at the cell boundary, which can be regarded as the Donnan potential, $\Phi_D \equiv \Phi(R)$. This yields the Debye–Hückel approximation $\Phi_\ell''(r) + 2\Phi_\ell'(r)/r = \kappa^2 \Phi_\ell'(r)$ for the shifted potential $\Phi_\ell(r) \equiv (\Phi(r) - \Delta\Phi)$, with $\Delta\Phi = \Phi_D - \tanh \Phi_D$, and the screening parameter $\kappa = \kappa_{\mathrm{res}} \sqrt{\cosh \Phi_D}$. Analytical solutions to the linearized PB equation are $\Phi_\ell(r) = a_+ e^{+\kappa r}/r + a_- e^{-\kappa r}/r$. These form an accurate approximation to the nonlinear profile in the proximity of the cell's boundary if one chooses $a_\pm = \exp(\mp \kappa R) \tanh \Phi_D (\kappa R \pm 1)/(2\kappa)$, where the latter follows from the constraints $\Phi_\ell(R) + \Delta\Phi = \Phi_D$ and $\Phi_\ell'(R) = 0$. The effective surface charge can now be extracted from the derivative of the analytical approximation at $r = a$, i.e., $Z^* \equiv -\Phi_\ell'(a) a^2/\lambda_B$ (see Fig. 1F), and one finds $Z^* = a_+/\lambda_B (\kappa a - 1) e^{+\kappa a} - a_-/\lambda_B (\kappa a + 1) e^{-\kappa a}$ (43). Then, using κ and Z^* as parameters, the effective interactions between the macroions can be estimated by using the DLVO theory again.

The accuracy and simplicity of the previous cell model approach can, however, be improved by calculating an effective point charge Q directly through identification of a point charge at $r = 0$ by extrapolating the analytical approximation (see Fig. 1G), yielding the form $Q \equiv \lim_{r \to 0} -\Phi_\ell'(r) r^2/\lambda_B = (a_+ + a_-)/\lambda_B$. The latter can also be expressed as

$$Q = \frac{\tanh \Phi_D}{\kappa \lambda_B} [\kappa R \cosh \kappa R - \sinh \kappa R]. \qquad [3]$$

The parameters κ and Q can then be used to approximate the effective electrostatic interactions in the original macroion system by those of point charges, using Eq. **1** to find the pairwise interaction energy. Although high macroion volume fractions
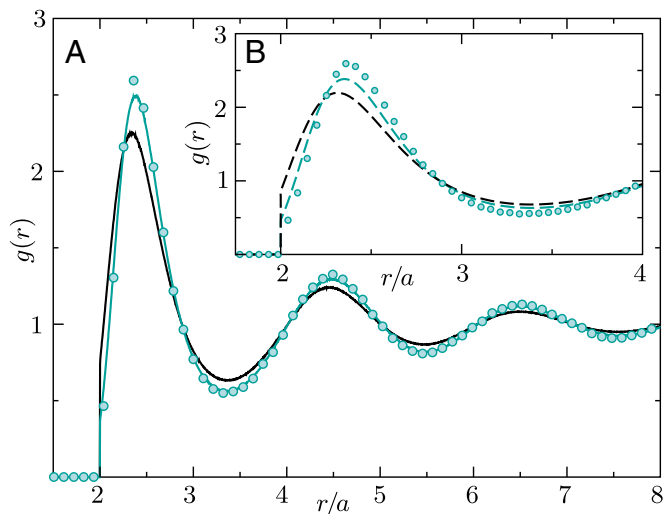
Fig. 2. Comparison of the pair correlation between macroions resulting from the full-ion PM MD simulations (circles) with those obtained by using repulsive-core effective screened Coulomb models (lines), relying on the EPC approach (green) and surface charge renormalization approach (black). The solid lines in *A* represent MD simulations results, whereas the dashed lines in *B* were obtained from the Ornstein–Zernike equation within the RY closure; both *A* and *B* correspond to the same system in which the valence and packing fraction of the macroions in the PM are $Z = 80$ and $\eta = 0.3682$, respectively.

render DLVO-based approaches inaccurate (21–25), the effective system of point charges has no hard-core volumes that will overlap with ionic double layers. We therefore expect that Eq. **3** in combination with Eq. **1** will remain accurate even in dense macroion systems. Note that the hard-core repulsions for $D < 2a$ should be maintained for the nonelectrostatic part of the pair interactions. Hereafter, we refer to the latter approach as the extrapolated point charge (EPC) method. The theoretical motivation for this approach is that screened Coulomb or Yukawa potentials solve the screened Poisson equation without considering the hard-core contribution of macroions at finite concentration. Thus, the main advantage of the EPC method is that it defines effective point charges in a consistent way, taking into account the excluded volume of highly charged macroions at any concentration.

In the regime where Z is small and the resulting potential profile is sufficiently flat throughout the cell, $|\Phi(R) - \Phi(a)| \ll 1$, the analytical approximations to Eq. **3** will become exact on the entire space between the cell boundary and the macroion surface. As a consequence, $a_\pm$ can be calculated from $\Phi_\ell(a) = -Z\lambda_B/a^2$ and $\Phi_\ell(R) = 0$, and a direct analytical relation between Z and Q follows (Fig. 1*D*). Tantalizingly, inserting this Q into Eq. **1** yields a pair potential similar to the DLVO equation,

$$\frac{U(D)}{k_B T} = \frac{Z^2 \lambda_B e^{-\kappa D} \left[2 e^{-\kappa(R-a)}(\kappa R \cosh \kappa R - \sinh \kappa R)\right]^2}{D\left[(1 + \kappa a)(\kappa R - 1) + (1 - \kappa a)(\kappa R + 1)e^{-2\kappa(R-a)}\right]^2}, \quad [4]$$

for $D \geq 2a$, and $V(D) = \infty$ for $D < 2a$. The screening parameter κ that enters Eq. **4** reduces to the reservoir value κ_{res} for systems with a sufficient amount of added salt, for which $|\Phi_D| \ll 1$. Recall that $R = a\eta^{-1/3}$ and that classical (η-independent) DLVO theory is reobtained for dilute suspensions, which is the limit $R \to \infty$. For completeness, we confirm that in the limit of large double-layer size, $\kappa^{-1} \gg D$, Eq. **4** reduces to the Coulombic form $U(D)/k_B T = (Z/(1-\eta))^2 \lambda_B/D$, with an effective charge $Z/(1-\eta)$ that is larger than the bare charge Z due to the expulsion of the ionic background from the hard core (26, 27, 44–46).

To verify our proposed prescription, molecular dynamic (MD) simulations of macroion/microion mixtures with particle diameters $d_M = 2a = 750$ Å and $d_+ = d_- = 3$ Å, respectively, were performed in the constant number, volume, and temperature (NVT) ensemble using the Large-scale Atomic/Molecular Massively Parallel Simulator (LAMMPS) package (47). This extreme size asymmetry between macroions and microions is selected to mimic realistic experimental colloidal systems. Macroions and monovalent microions, fulfilling the electroneutral condition, were placed inside a cubic simulation box of length L under periodic boundary conditions. In the PM representation that we applied here, ionic species are represented by repulsive-core spheres with point charges in their centers immersed in a continuous solvent (48–51). The pairwise forces among all particles have a short-range repulsive-core potential component, $u_{ij}^{rc}(D)$, and a long-range Coulombic pair potential contribution, $u_{ij}^{el}(D)/k_B T = \lambda_B z_i z_j/D$, where z_i and z_j are the valences associated to particles i and j, respectively. These interactions are handled properly, using the particle mesh Ewald technique (52). We model the repulsive-core pair potential between a particle of species i and a particle of species j, separated by a distance D, as an impenetrable hard-core $u_{ij}^{rc}(D) = \infty$ for $D \leq \Delta_{ij}$, a shifted–truncated Lennard–Jones potential $u_{ij}^{rc}(D)/k_B T = 4[(\sigma/(D - \Delta_{ij}))^{12} - (\sigma/(D - \Delta_{ij}))^6] + 1$ for $\Delta_{ij} < D < \Delta_{ij} + 2^{1/6}\sigma$, and by a potential $u_{ij}^{rc}(D) = 0$ for $D \geq \Delta_{ij} + 2^{1/6}\sigma$, where $\Delta_{ij} = (d_i + d_j)/2 - \sigma$ is the hard-core diameter. The parameter σ regulates the hardness of the repulsive-core interactions. To mimic the hard-core interaction characteristic of the PM, σ is set equal to 0.1 nm. We use $\lambda_B = 7.143$ Å throughout the text for theoretical and simulation calculations. Additional details of the simulation setup can be found in refs. 49–51.

Results

In Fig. 2, we compare radial distributions from computationally expensive PM MD simulations (circles) to much faster and more economic effective-model descriptions using MD simulations (solid lines), and integral equations (Fig. 2*B*, dashed lines). In the PM approach, we use a cubic simulation box of length $L = 8d_M = 6,000$ Å, containing 360 macroions of valence $Z = 80$, 31,680 small monovalent counterions ($-e$), and 2,880 small
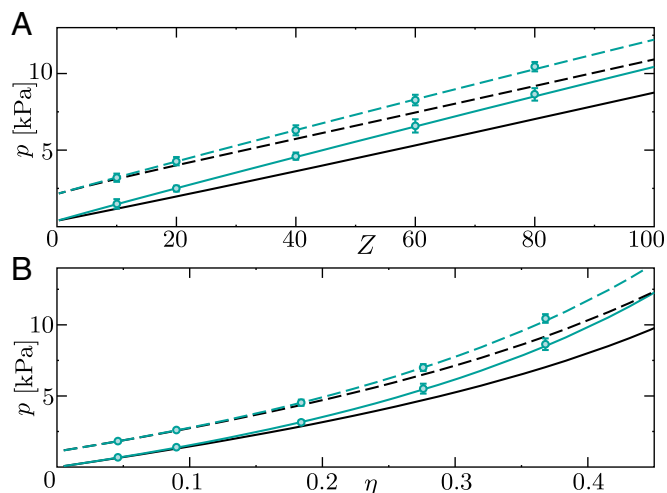
Fig. 3. The total pressure in the macroion/microion mixture as a function of (*A*) Z for a fixed macroion volume fraction $\eta = 0.3682$, and as a function of (*B*) η and for $Z = 80$. Both graphs show data for both the salt-free (solid, lower set of lines and circles) and the added-salt case (dashed, upper set of lines and circles), in which 2,880 extra cations and 2,880 extra anions were added. The lines result from RY calculations using the effective model parameters following from the EPC approach (green) or surface charge renormalization approach (black). The circles show the results of PM simulations, and error bars are included for those cases where the error is larger than the circle size.

monovalent coions ($+e$). In the effective-model approach, microions are included implicitly in the Yukawa interactions between macroions with an effective charge Q and inverse screening length κ. The charges associated to the macroion profiles shown in Fig. 2 are $Q = 204$ following the EPC approach and $Q = 167$ following the surface charge renormalization approach in combination with the DLVO theory. An excellent agreement between the heavy-duty PM results, in which microions are included explicitly, and the computationally inexpensive MD Yukawa simulations using the EPC prescription can be observed in Fig. 2A. In contrast, surface charge renormalization in combination with the DLVO theory deviates significantly from PM simulation results, as expected at this volume fraction. The use of integral equations theory allows for an even faster numerical calculation of the radial distribution functions within the effective model. The Rogers–Young (RY) closure (53), which is known for its superb accuracy for hard-core Yukawa systems (46, 54–56), has good qualitative agreement compared with PM results, as seen in Fig. 2B. Note that PB techniques are grand canonical and therefore require a reservoir ion density c_s or screening parameter κ_{res}, while the number of ions in the PM system is fixed, as there is no particle exchange with a reservoir. Therefore, we add an additional step to our PB method to obtain canonical results: for any choice of c_s, we integrate the resulting ion profiles in the cell, which yields the total number of ions per macroion. The latter can be compared with the number of ions per macroion in the simulation box. Subsequently, the right value for c_s is determined by a root-finding procedure with respect to their difference.

The total microion/macroion pressure resulting from the PM, p_{PM}, as well as the macroion pressure in the effective model, p_{EM}, can be calculated via the virial equation $p = (N/V)k_B T + (1/3V)\langle \sum_{i<j}^{N} D_{ij} \cdot U'_{ij}(D_{ij}) \rangle$, where N sums all particles, in the PM, or only the macroions, in the effective model, and $U'_{ij}(D_{ij})$ is the derivative with respect to the distance D_{ij} of the (un)screened Coulomb pair interaction between particles i and j. However, to relate p_{EM} to p_{PM}, it is essential to include a correction term that can be regarded as the pressure of a homogeneous background of counterions and coions,

$$p_{PM} \approx p_{EM} + k_B T \frac{\kappa^2}{8\pi\lambda_B}\left(1 + \frac{\kappa_{res}^4}{\kappa^4}\right). \qquad [5]$$

Density functional theory (21, 22, 25, 57) may be applied for a rigorous derivation of this pressure difference, which shows up as a volume term in the free energy of the effective system (22, 58–60). We refer to *SI Text* for this. Note that Eq. **5** implies that the macroion osmotic pressure, which is the pressure with respect to the ion reservoir, $\Pi = p_{PM} - 2c_s k_B T$ (34), does not equal p_{EM} in general; only if κ approaches κ_{res} does the pressure difference in Eq. **5** reduce to $k_B T \kappa_{res}^2/(4\pi\lambda_B) = 2c_s k_B T$.

Fig. 3 shows the PM pressure p_{PM} resulting from PM simulations, as well as the effective-model approximations following from Eq. **5** applying the RY closure. Even though the agreement between the radial distribution functions obtained from the EPC method using the RY closure and the PM simulations is not as accurate as that obtained from the EPC effective screened Coulomb simulations (see, e.g., Fig. 2), we have observed that the virial pressure obtained from the RY closure and the

effective screened Coulomb simulations using the EPC approach agreed with the pressure p_{PM} obtained from the PM simulations within the corresponding numerical uncertainty. One observes superior accuracy of EPC with respect to the surface charge renormalization approach for a wide range in Z (Fig. 3A), and in particular for high η (Fig. 3B). While the dashed lines in Fig. 3 represent added salt cases, the full lines correspond to a system without coions, i.e., a salt-free "reservoir": $c_s = \kappa_{res}^2/(8\pi\lambda_B) = 0$ (61, 62), for which Eqs. **2a** and **2b** in principle cannot be solved. Our cell calculations, however, show that the salt-free limit $\kappa_{res} \to 0$ is perfectly well defined and can be characterized by the condition that the number of coions is negligible with respect to the counterions. For small κ_{res}, all relevant physical quantities such as the number of ions per macroion, Q, and κ converge to their values in a salt-free environment. Salt-free cases therefore do not require a root-finding procedure with respect to κ_{res}, but instead can be considered by choosing κ_{res} sufficiently small such that $\kappa_{res}/\kappa \ll 1$, i.e., $\Phi_D \gg 1$. For small macroion charges, $Z\lambda_B/a < 1$, we find that the resulting physical κ is in accordance with a homogeneous distribution of neutralizing counterions, $\kappa^2 = 3Z\lambda_B\eta/(a^3(1-\eta))$ (21, 44, 45, 62). This, in combination with Eq. **4**, yields a description at any density of the pair interactions in salt-free systems depending on Z, λ_B, a, and η only. The pressure correction in Eq. **5** reduces to $k_B T \kappa^2/8\pi\lambda_B$. The strong dependence of κ on η, is particularly important in other geometries, such as the charged two-plate system, from what we study here. In the latter, the distance between the plates also sets the system's volume and therefore κ, yielding a nonexponential form for the pair potential (63). However, for macroion suspensions this is not the case, as η is a fixed parameter independent of the configuration.

Conclusions

In this work, we have introduced a method that extends the capabilities of the DLVO theory to high valences and volume fractions of colloidal macroions using no additional assumptions besides the underlying PB theory. Akin to the original theory, this approach is mainly applicable to systems with monovalent microions for which ion correlations are unimportant, although approximate extensions to systems with correlated multivalent counterions might be obtainable. We also propose a route to relate the pressure in the effective system of macroions to the osmotic pressure that can be measured experimentally in colloidal systems, for example, in sedimentation profiles (64, 65). Our method demonstrates accuracy with respect to acquiring the measurable properties of charged colloidal suspensions, and can therefore be applied to guide and interpret experiments on related systems.

1. Langmuir I (1938) The role of attractive and repulsive forces in the formation of tactoids, thixotropic gels, protein crystals and coacervates. *J Chem Phys* 6(12): 873–896.
2. Derjaguin B, Landau L (1941) Theory of the stability of strongly charged lyophobic sols and of the adhesion of strongly charged particles in solution of electrolytes. *Acta Physicochim. URSS* 14:633–662.
3. Verwey EJW, Overbeek JTG (1948) *Theory of the Stability of Lyophobic Colloids* (Elsevier, New York).
4. Levine S, Mingins J, Bell G (1967) The discrete-ion effect in ionic double-layer theory. *J Electroanal Chem Interfacial Electrochem* 13(3):280–329.
5. Stillinger FH, Jr, Kirkwood JG (1960) Theory of the diffuse double layer. *J Chem Phys* 33(5):1282–1290.

6. Levine S, Outhwaite CW, Bhuiyan LB (1981) Statistical mechanical theories of the electric double layer. *J Electroanal Chem Interfacial Electrochem* 123(1):105–119.
7. Blum L (1977) Theory of electrified interfaces. *J Phys Chem* 81(2):136–147.
8. Valleau J, Ivkov R, Torrie G (1991) Colloid stability: The forces between charged surfaces in an electrolyte. *J Chem Phys* 95(1):520–532.
9. Oosawa F (1971) *Polyelectrolytes* (Marcel Dekker, New York).
10. Henderson D (1992) The interaction between macrospheres in solution. *Fluid Phase Equilib* 76(21):1–9.
11. Chu X, Wasan DT (1996) Attractive interaction between similarly charged colloidal particles. *J Colloid Interface Sci* 184(1):268–278.
12. Netz RR, Orland H (2000) Beyond Poisson-Boltzmann: Fluctuation effects and correlation functions. *Eur Phys J E* 1:203–214.

13. Panagiotopoulos AZ, Fisher ME (2002) Phase transitions in 2:1 and 3:1 hard-core model electrolytes. *Phys Rev Lett* 88(4):045701.
14. Kjellander R (2010) Ion-ion correlations and effective charges in electrolyte and macroion systems. *Ber Bunsenges Phys Chem* 100(6):894–904.
15. Wernersson E, Kjellander R, Lyklema J (2010) Charge inversion and ion-ion correlation effects at the mercury/aqueous MgSO$_4$ interface: Toward the solution of a long-standing issue. *J Phys Chem C* 114(4):1849–1866.
16. Zwanikken JW, Olvera de la Cruz M (2013) Tunable soft structure in charged fluids confined by dielectric interfaces. *Proc Natl Acad Sci USA* 110(14):5301–5308.
17. Ninham B (1999) On progress in forces since the DLVO theory. *Adv Colloid Interface Sci* 83(1-3):1–17.
18. Glendinning A, Russel W (1983) The electrostatic repulsion between charged spheres from exact solutions to the linearized Poisson-Boltzmann equation. *J Colloid Interface Sci* 94(1):95–104.
19. Carnie SL, Chan DY, Stankovich J (1994) Computation of forces between spherical colloidal particles: Nonlinear Poisson–Boltzmann theory. *J Colloid Interface Sci* 165(1):116–128.
20. Warszyński P, Adamczyk Z (1997) Calculations of double-layer electrostatic interactions for the sphere/plane geometry. *J Colloid Interface Sci* 187(2):283–295.
21. von Grünberg HH, van Roij R, Klein G (2001) Gas-liquid phase coexistence in colloidal suspensions? *Europhys Lett* 55(4):580–586.
22. van Roij R, Hansen JP (1997) Van der Waals–like instability in suspensions of mutually repelling charged colloids. *Phys Rev Lett* 79(16):3082–3085.
23. Warren PB (2000) A theory of void formation in charge-stabilized colloidal suspensions at low ionic strength. *J Chem* 112(10):4683–4698.
24. Löwen H, Madden PA, Hansen JP (1992) Ab initio description of counterion screening in colloidal suspensions. *Phys Rev Lett* 68(7):1081–1084.
25. Hansen JP, Löwen H (2000) Effective interactions between electric double layers. *Annu Rev Phys Chem* 51:209–242.
26. Marcelja S, Mitchell D, Ninham B (1976) Phase transitions in aqueous suspensions of spherical colloid particles. *Chem Phys Lett* 43(2):353–357.
27. Kanai T, et al. (2015) Crystallization and reentrant melting of charged colloids in nonpolar solvents. *Phys Rev E Stat Nonlin Soft Matter Phys* 91(3):030301.
28. Stigter D (1954) On the thermodynamics of micellar solutions. *Recl Trav Chim Pays Bas* 73(7):593–610.
29. van Megen W, Snook I (1975) A hard sphere model for order-disorder transitions in colloidal dispersions. *Chem Phys Lett* 35(3):399–402.
30. Brenner SL (1976) A semiempirical model for the phase transition in polystyrene latexes. *J Phys Chem* 80(13):1473–1477.
31. Beunen JA, White LR (1981) The order-disorder transition in latex dispersions. *Colloids Surf* 3(4):371–390.
32. Trizac E, Levin Y (2004) Renormalized jellium model for charge-stabilized colloidal suspensions. *Phys Rev E Stat Nonlin Soft Matter Phys* 69(3 Pt 1):031403.
33. Alexander S, et al. (1984) Charge renormalization, osmotic pressure, and bulk modulus of colloidal crystals: Theory. *J Chem Phys* 80(11):5776–5781.
34. Reus V, Belloni L, Temb T, Lutterbach N, Versmold D (1997) Equation of state and structure of electrostatic colloidal crystals: Osmotic pressure and scattering study. *J. Phys. II France* 7(4):603–626.
35. Griffiths D (1999) *Introduction to Electrodynamics* (Prentice Hall, Upper Saddle River, NJ), Vol 3.
36. Dobnikar J, Chen Y, Rzehak R, von Grünberg HH (2003) Many-body interactions and the melting of colloidal crystals. *J Chem Phys* 119(9):4971–4985.
37. Dobnikar J, Castañeda Priego R, von Grünberg HH, Trizac E (2006) Testing the relevance of effective interaction potentials between highly-charged colloids in suspension. *New J Phys* 8:277.
38. Belloni L (1997) Ionic condensation and charge renormalization in colloidal suspensions. *Colloids Surf A Physicochem Eng Asp* 140(1-3):227–243.
39. Trizac E, Bocquet L, Aubouy M (2002) Simple approach for charge renormalization in highly charged macroions. *Phys Rev Lett* 89(24):248301.
40. Trizac E, Bocquet L, Aubouy M, von Grünberg HH (2003) Alexander's prescription for colloidal charge renormalization. *Langmuir* 19(9):4027–4033.
41. Diehl A, Levin Y (2004) Effective charge of colloidal particles. *J Chem Phys* 121(23):12100–12103.
42. Denton AR (2010) Poisson-Boltzmann theory of charged colloids: Limits of the cell model for salty suspensions. *J Phys Condens Matter* 22(36):364108.
43. Zoetekouw B (2006) Phase behaviour of charged colloids: Many-body effects, charge renormalization, and charge regulation. PhD thesis (Utrecht University, Utrecht, Netherlands).
44. Russel WB, Benzing DW (1981) The viscoelastic properties of ordered latices: A self-consistent field theory. *J Colloid Interface Sci* 83(1):163–177.
45. Denton AR (2000) Effective interactions and volume energies in charged colloids: linear response theory. *Phys Rev E Stat Phys Plasmas Fluids Relat Interdiscip Topics* 62:(3 Pt B):3855–3864.
46. Heinen M, Holmqvist P, Banchio AJ, Nägele G (2011) Pair structure of the hard-sphere Yukawa fluid: An improved analytic method versus simulations, Rogers-Young scheme, and experiment. *J Chem Phys* 134(4):044532.
47. Plimpton S (1995) Fast parallel algorithms for short-range molecular dynamics. *J Comput Phys* 117(1):1–19.
48. Hynninen AP, Dijkstra M (2005) Melting line of charged colloids from primitive model simulations. *J Chem Phys* 123(24):244902.
49. González-Mozuelos P, Guerrero-García GI, Olvera de la Cruz M (2013) An exact method to obtain effective electrostatic interactions from computer simulations: The case of effective charge amplification. *J Chem Phys* 139(6):064709.
50. Guerrero-García GI, González-Mozuelos P, Olvera de la Cruz M (2013) Large counterions boost the solubility and renormalized charge of suspended nanoparticles. *ACS Nano* 7(11):9714–9723.
51. Guerrero García GI, Olvera de la Cruz M (2014) Polarization effects of dielectric nanoparticles in aqueous charge-asymmetric electrolytes. *J Phys Chem B* 118(29):8854–8862.
52. Darden T, York D, Pedersen L (1993) Particle mesh Ewald: An $N \cdot \log (N)$ method for Ewald sums in large systems. *J Chem Phys* 98(12):10089–10092.
53. Rogers FJ, Young DA (1984) New, thermodynamically consistent, integral equation for simple fluids. *Phys Rev A* 30(2):999–1007.
54. Castañeda-Priego R, Rojas-Ochoa LF, Lobaskin V, Mixteco-Sánchez JC (2006) Macroion correlation effects in electrostatic screening and thermodynamics of highly charged colloids. *Phys Rev E Stat Nonlin Soft Matter Phys* 74(5 Pt 1):051408.
55. Gapinski J, Nägele G, Patkowski A (2012) Freezing lines of colloidal Yukawa spheres. I. A Rogers-Young integral equation study. *J Chem Phys* 136(2):024507.
56. Zhou S, Zhang X (2003) Freezing of charge-stabilized colloidal dispersions. *J Phys Chem B* 107(22):5294–5299.
57. Evans R (1979) The nature of the liquid-vapour interface and other topics in the statistical mechanics of non-uniform, classical fluids. *Adv Phys* 28(2):143–200.
58. Graf H, Löwen H (1998) Density jumps across phase transitions in soft matter systems. *Phys Rev E Stat Phys Plasmas Fluids Relat Interdiscip Topics* 57(5):5744–5753.
59. Zoetekouw B, van Roij R (2006) Volume terms for charged colloids: A grand-canonical treatment. *Phys Rev E Stat Nonlin Soft Matter Phys* 73(2 Pt 1):021403.
60. Zoetekouw B, van Roij R (2006) Nonlinear screening and gas-liquid separation in suspensions of charged colloids. *Phys Rev Lett* 97(25):258302.
61. Sainis SK, Merrill JW, Dufresne ER (2008) Electrostatic interactions of colloidal particles at vanishing ionic strength. *Langmuir* 24(23):13334–13337.
62. Ohshima H (2002) Surface charge density/surface potential relationship for a spherical colloidal particle in a salt-free medium. *J Colloid Interface Sci* 247(1):18–23.
63. Briscoe WH, Attard P (2002) Counterion-only electrical double layer: A constrained entropy approach. *J Chem Phys* 117(11):5452–5464.
64. Torres A, Cuetos A, Dijkstra M, van Roij R (2008) Breakdown of the Yukawa model in de-ionized colloidal suspensions. *Phys Rev E Stat Nonlin Soft Matter Phys* 77(3 Pt 1):031402.
65. Royal CP, van Roij R, van Blaaderen A (2005) Extended sedimentation profiles in charged colloids: The gravitational length, entropy, and electrostatics. *J Phys Condens Matter* 17(15):2315.